

# Finger formation at the base of ash clouds: A linear stability analysis



UNIVERSITÉ  
DE GENÈVE

Paul Jarvis <sup>1</sup> Jonathon Lemus <sup>1</sup> Allan Fries <sup>1</sup>  
Amanda Clarke <sup>2</sup> Jeremy Phillips <sup>3</sup> Costanza Bonadonna <sup>1</sup>

<sup>1</sup>Section of Earth and Environmental Sciences, University of Geneva

<sup>2</sup>School of Earth and Space Exploration, Arizona State University

<sup>3</sup>School of Earth Sciences, University of Bristol

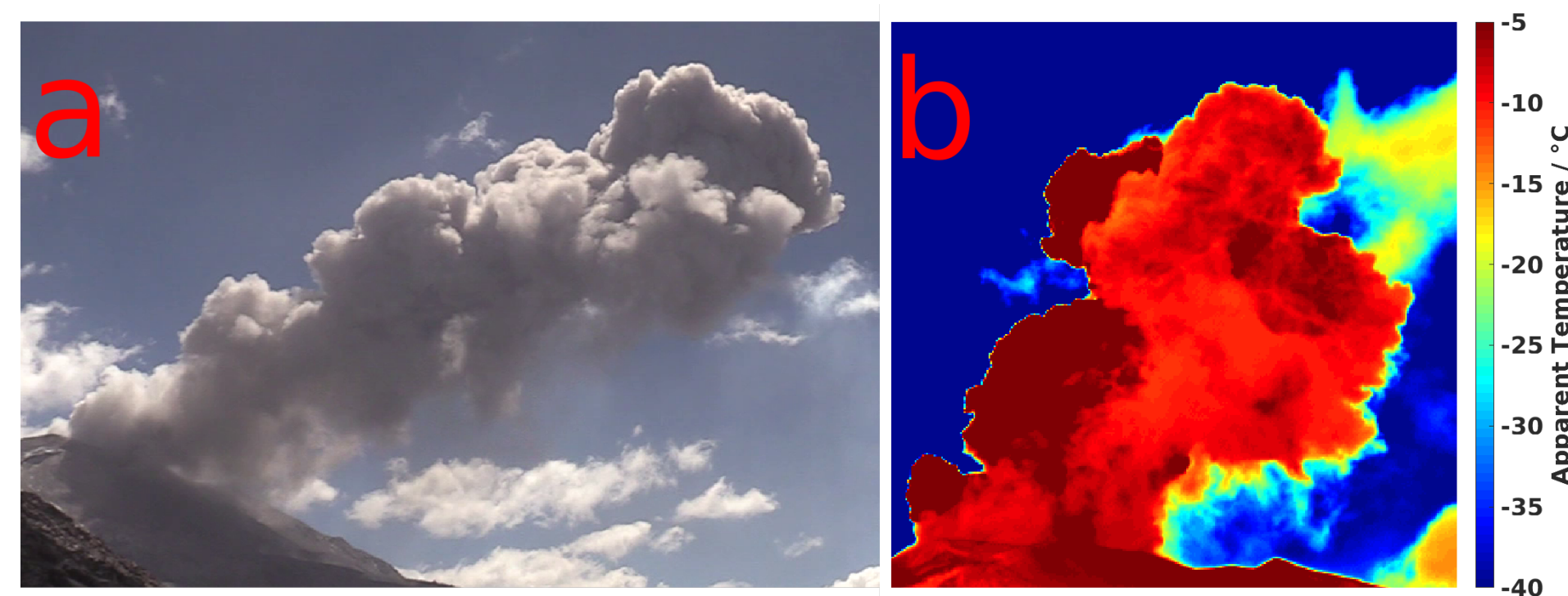


Figure 1. a) Visible and b) infrared images of ash clouds from Vulcanian explosions of Sabancaya volcano, Peru. Fingers can be seen in both images.

## Introduction

Volcanic ash presents a hazard for infrastructure and human health. Understanding ash settling is therefore crucial for assessing the associated risk. Downward-propagating fingers (Figures 1 and 2), hypothesised to form from a gravitational instability at the base of the ash cloud have been seen at many volcanoes, and in analogue experiments<sup>1,2</sup> (Allan Fries) and numerical models<sup>3</sup> (Jonathon Lemus). Here we present a linear stability analysis, that predicts the initial growth rate of the fingers.

We model the ash cloud as a particle suspension overlying a denser fluid (salt or sugar water in experiments; Figure 3). As particles settle towards the interface, a narrow ash-rich, gravitationally unstable layer forms called the particle boundary layer (Figure 4). Small disturbances in this layer rapidly grow to form fingers, which propagate downwards faster than the settling velocity of individual particles, impacting fine ash dispersal.

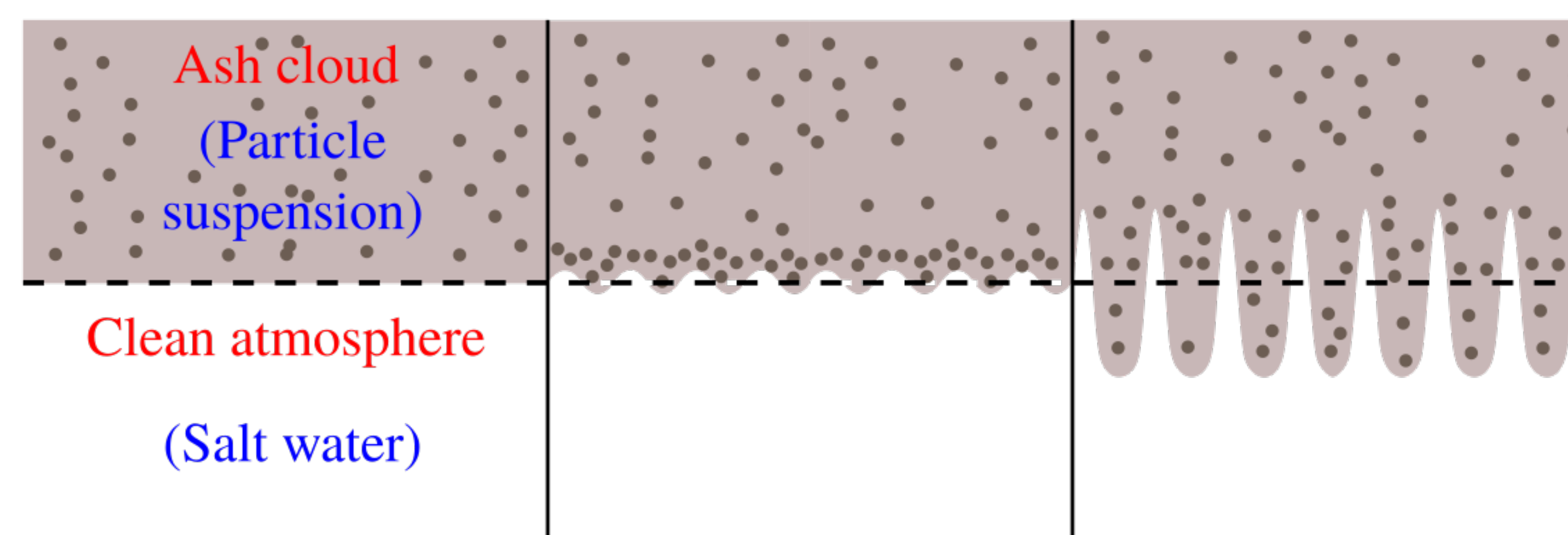


Figure 3. Schematic showing the formation of fingers at base of an ash cloud.

## Equations of motion

Conservation of mass

$$\nabla \cdot \mathbf{u}(\mathbf{x}, t)$$

$$\mathbf{u}(\mathbf{x}, t) = \hat{\mathbf{u}}(z)e^{i(k_x x + k_y y - \omega t)}$$

Conservation of momentum

$$\frac{\partial \mathbf{u}(\mathbf{x}, t)}{\partial t} + [\mathbf{u}(\mathbf{x}, t)] \cdot \nabla \mathbf{u}(\mathbf{x}, t) = \frac{\nabla P(\mathbf{x}, t)}{\rho_0} + \nu \nabla^2 \mathbf{u}(\mathbf{x}, t) - g' \hat{\mathbf{z}} \quad P(\mathbf{x}, t) = P^{(0)}(\mathbf{x}, t) + \hat{P}(z)e^{i(kx - \omega t)}$$

Conservation of particles

$$\frac{\partial \phi(\mathbf{x}, t)}{\partial t} + [\mathbf{u}(\mathbf{x}, t)] - \mathbf{U}_p \cdot \nabla \phi(\mathbf{x}, t) = D_p \nabla^2 \phi(\mathbf{x}, t) \quad \phi(\mathbf{x}, t) = \phi^{(0)}(\mathbf{x}, t) + \hat{\phi}(z)e^{i(kx - \omega t)}$$

Conservation of solute

$$\frac{\partial s(\mathbf{x}, t)}{\partial t} + \mathbf{u}(\mathbf{x}, t) \cdot \nabla s(\mathbf{x}, t) = D_s \nabla^2 s(\mathbf{x}, t) \quad s(\mathbf{x}, t) = s^{(0)}(\mathbf{x}, t) + \hat{s}(z)e^{i(kx - \omega t)}$$

Reduced gravity

$$g' = g \left( 1 + \alpha s(\mathbf{x}, t) + \frac{\rho_p \phi(\mathbf{x}, t)}{\rho_0} \right)$$

$$\hat{P} \ll P^{(0)}, \hat{\phi} \ll \phi^{(0)}, \hat{s} \ll s^{(0)}$$

## Base states

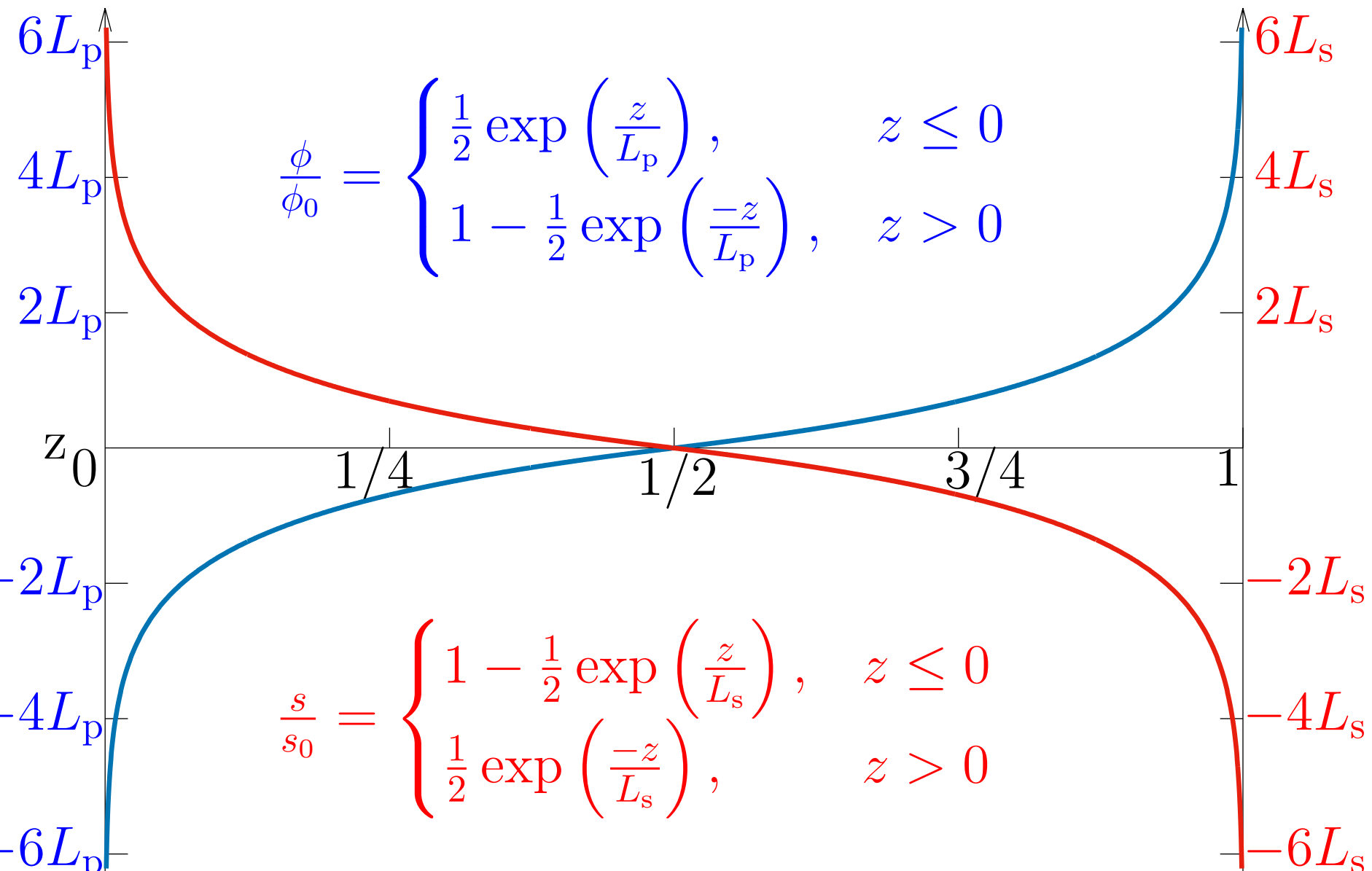


Figure 5. Choice of base states for the particle and solute concentrations. The transitions have length scales  $L_p$  and  $L_s$  respectively.

To validate the model, we consider the special case of a single phase ( $s_0 = 0$ ) in the absence of a settling velocity ( $U_p' = 0$ ). This reduces the problem to that of the well studied Rayleigh-Taylor case<sup>5</sup>.

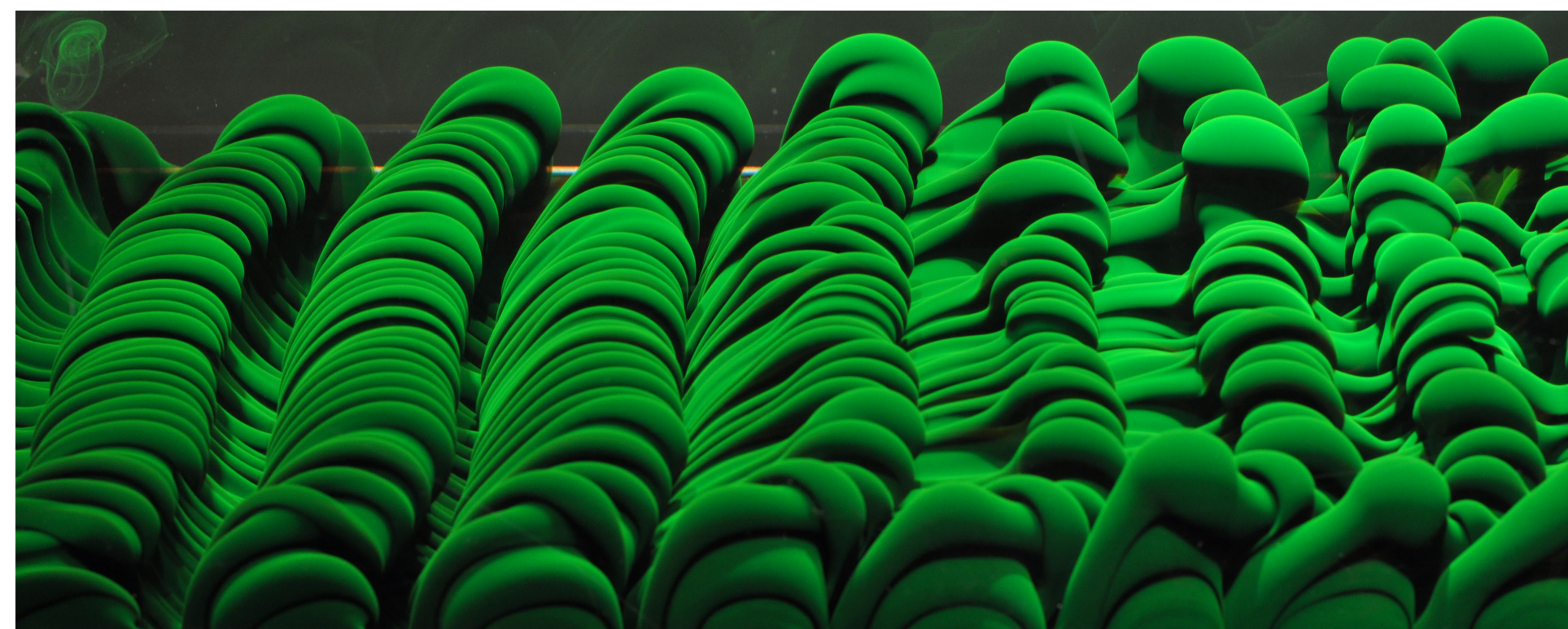


Figure 6. Experimentally produced Rayleigh-Taylor instability. The green fluid is lighter than the overlying clear fluid. Credit: Megan Davies Wykes

Choose sufficiently large  $Re(10^4)$  and  $Sc_p(10^3)$  that system becomes independent of them.

## Further work

- Include non-zero settling velocity  $U_p$
- Account for presence of solute ( $s_0 \neq 0$ )
- Include non-zero velocity base state and study effect of shear
- Compare results with simulations and experiments (Figure 8)

## References

1) Manzella et al. 2015, Geology 43

2) Scoll et al. 2017, Bull. Volcanol. 79

3) Burns and Melburg 2015, J. Fluid Mech. 762

4) Burns and Melburg 2012, J. Fluid Mech. 691

5) Chandrasekhar 1961, *Hydrodynamic and Hydromagnetic Stability*

## Expansion



Figure 2. Fingers seen in ash clouds at a) Etna 2013 and b) Eyjafjallajökull 2010. Adapted from Scoll et al. 2017.

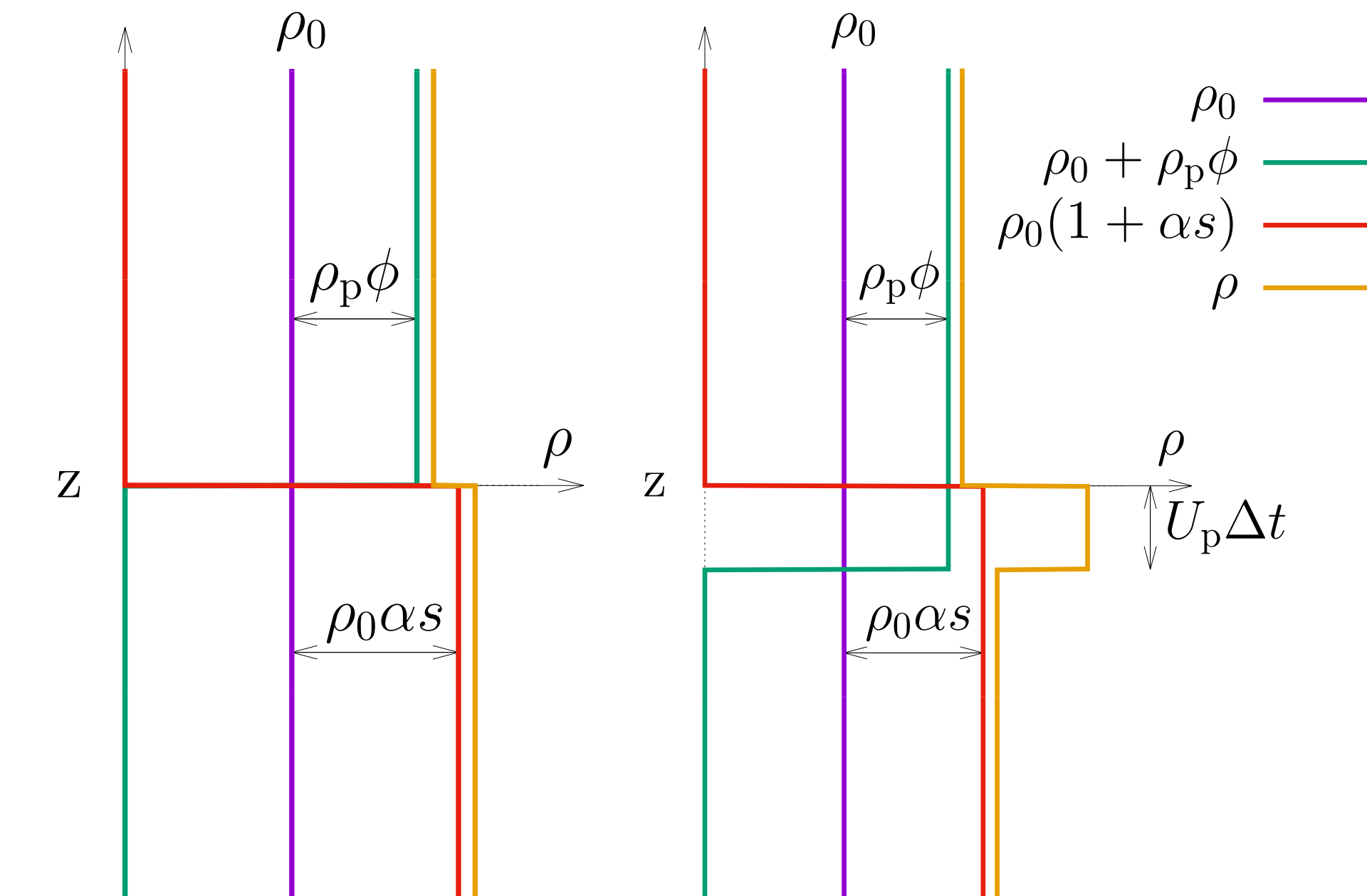


Figure 4. Despite an initial stable configuration, ash settling leads to the formation of a gravitationally unstable particle boundary layer.

Unknowns		Parameters	
$\mathbf{u}(\mathbf{x}, t)$	Fluid velocity	$\rho_0$	Reference fluid density
$P(\mathbf{x}, t)$	Pressure	$\nu$	Kinematic viscosity
$\phi(\mathbf{x}, t)$	Particle volume	$\mathbf{U}_p$	Particle settling velocity
$s(\mathbf{x}, t)$	Solute concentration	$\rho_p$	Particle density
Variables		Variables	
$\mathbf{x}$	Position vector	$D_p$	Particle diffusivity
$t$	time	$D_s$	Solute diffusivity
$\hat{\mathbf{z}}$	Vertical unit vector	$g$	Gravity
		$\alpha$	Expansivity

## Non-dimensionalisation and generalised eigenvalue problem

This gives eight dimensionless parameters

$$\begin{aligned} Re &= \frac{gL_p^3}{\nu^2} & U_p' &= \frac{\nu U_p}{gL_p^2} & L_s' &= \frac{L_s}{L_p} & \phi_0 \\ A_\beta &= \frac{\alpha s_0 \nu^2}{gL_p^3} & A_\gamma &= \frac{\rho_p \nu^2}{gL_p^3 \rho_0} & Sc_s &= \frac{\nu}{D_s} & Sc_p &= \frac{\nu}{D_p} \end{aligned}$$

Can express problem as a generalised eigenvalue equation

$$\begin{pmatrix} \frac{1}{Re} \left( \frac{d^4}{dz^4} - 2k'^2 \frac{d^2}{dz^2} + k'^4 \right) & k'^2 A_\beta & k'^2 A_\gamma & \hat{u}_z' \\ \frac{\partial s^{(0)}}{\partial z'} & Re Sc_s \left( k'^2 - \frac{d^2}{dz^2} \right) & 0 & \hat{s}' \\ \frac{\partial \phi^{(0)}}{\partial z'} & 0 & Re Sc_p \left( k'^2 - \frac{d^2}{dz^2} \right) - U_p' \frac{d}{dz'} & \hat{\phi}' \end{pmatrix} \begin{pmatrix} \hat{u}_z' \\ \hat{s}' \\ \hat{\phi}' \end{pmatrix} = i\omega' \begin{pmatrix} \left( k'^2 - \frac{d^2}{dz^2} \right) & 0 & 0 \\ 0 & 1 & 0 \\ 0 & 0 & 1 \end{pmatrix} \begin{pmatrix} \hat{u}_z' \\ \hat{s}' \\ \hat{\phi}' \end{pmatrix}$$

This is a generalised eigenvalue problem<sup>4X</sup> and is solved for the eigenvalue  $\omega' = \Omega + i\sigma'$ . Solutions where  $\sigma' < 0$  are unstable, and the associated growth rate is  $|\sigma'|$ . We can therefore predict the fastest growing perturbation wavelength  $\lambda_{\max} = 2\pi/k_{\max}$  which maximises  $|\sigma'|$  for different values of the dimensionless parameters.

## Special case: Rayleigh-Taylor instability

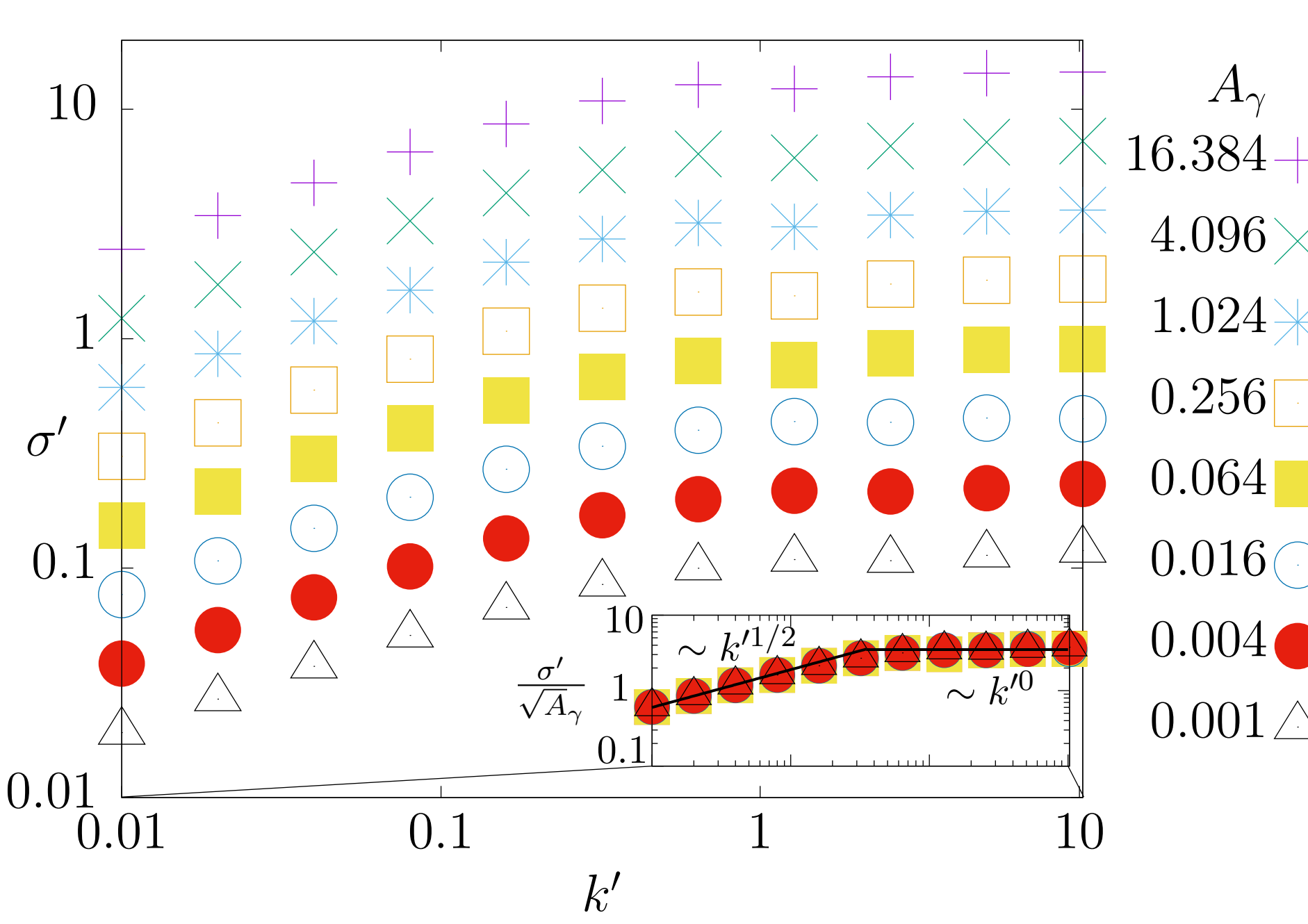


Figure 7. Dispersion relation showing that  $\sigma' \sim A_\gamma$ . There are two regimes of  $k'$  dependence, when  $k' < 1$ ,  $\sigma' \sim k'^{1/2}$  and when  $k' > 1$ ,  $\sigma' \sim k'^0$ .

## Conclusions

- Ash fingers are produced by a gravitational instability
- Linear stability analysis predicts fastest growing wavelength
- Code can reproduce Rayleigh-Taylor instability
- Can easily include other effects such as shear and diffusion

$k' < 1$  ( $\lambda > 2\pi L_p$ )

Wavelength is larger than the transition region. Scaling behaviour the same as for an infinitesimally thin transition zone.

$$\sigma' \sim \left( \frac{gk \rho_p}{\rho_0} \right)^{1/2}$$

$k' > 1$  ( $\lambda < 2\pi L_p$ )

Wavelength is shorter than the transition region. Growth rate independent of wavenumber.

$$\sigma' \sim \left( \frac{g \rho_p}{L_p \rho_0} \right)^{1/2}$$



Figure 8. Fingers formed under shear in preliminary experiments.